



Published in final edited form as:

Chemistry. 2015 September 21; 21(39): 13488–13500. doi:10.1002/chem.201501178.

## Circularly Polarized Luminescence from Simple Organic Molecules

Esther M. Sánchez-Carnerero<sup>[a]</sup>, Prof. Dr. Antonia R. Agarrabeitia<sup>[a]</sup>, Prof. Dr. Florencio Moreno<sup>[a]</sup>, Prof. Dr. Beatriz L. Maroto<sup>[a]</sup>, Prof. Dr. Gilles Muller<sup>[b]</sup>, Prof. Dr. María J. Ortiz<sup>[a]</sup>, and Prof. Dr. Santiago de la Moya<sup>[a]</sup>

Santiago de la Moya: santmoya@ucm.es

<sup>[a]</sup>Department of Organic Chemistry I, Universidad Complutense de Madrid, Facultad de Ciencias Químicas, Ciudad Universitaria s/n, Madrid, 28040, Spain

<sup>[b]</sup>Department of Chemistry, San José State University, One Washington Square, San José, CA 95192-0101, USA

### Abstract

This article aims to show the identity of “CPL-active simple organic molecules” as a new concept in Organic Chemistry due to the potential interest of these molecules, as availed by the exponentially growing number of research articles related to them. In particular, it describes and highlights the interest and difficulty in developing chiral simple (small and nonaggregated) organic molecules able to emit left- or right-circularly polarized light efficiently, the efforts realized up to now to reach this challenging objective, and the most significant milestones achieved to date. General guidelines for the preparation of these interesting molecules are also presented.

### Keywords

Circularly Polarized Luminescence; Small Organic Molecules; Chirality; Fluorescence; Chromophores

### Introduction

Two circular polarization states (left and right circular polarization) are possible for single photons, as a consequence of their quantum properties as uncharged, massless gauge bosons (quantized spin =  $\pm 1\hbar$ ).<sup>1</sup> In the right-circular polarization state, the associated electric and magnetic vectors describe a clock-wise helix, as the wave propagates towards the observer (right-circularly polarized wave), whereas for the left-circular polarization state the propagation of said vectors describes an anticlock-wise helix (left-circularly polarized wave).<sup>1</sup> Therefore, circular polarization confers to a beam of light (constituted for several photons) a chiral character, due to the helical chirality associated to the corresponding (left

Correspondence to: Santiago de la Moya, santmoya@ucm.es.

or right) propagation mode. This chiral characteristic is the basis of the chiral photonics, also known as chiral optics or simply *chiroptics*.<sup>2</sup>

The differential emission of right and left circularly polarized light by chiral nonracemic luminescent systems (molecules, ionic pairs, polymers, metal complexes, supramolecular aggregates, etc.) is known as *circularly polarized luminescence* (hereafter CPL).<sup>2</sup> The growing interest of this chiroptical phenomenon is mainly due to the resolution provided by the circular polarization, which allows the development of smarter photonic materials for advanced technologies, such as 3D displaying,<sup>3</sup> information storage and processing,<sup>4</sup> communication of spin information (spintronics-based devices),<sup>5</sup> or ellipsometry-based tomography.<sup>6</sup> Moreover, while spectroscopy based on the differential absorption of right and left circularly polarized light, known as *circular dichroism* (hereafter CD), can be used as a source of information about chiral structures at their ground states (chiral configurations or conformations), spectroscopy based on CPL is indispensable for studying the chirality of emitting excited states.<sup>7</sup>

As Faraday himself pointed out, polarized light is the “most subtle and delicate investigator of molecular condition”. In this line, resolution and dependence with chirality make CPL an ineludible source of information on chiral environments to be exploited. This kind of information is extremely valuable taking into account the omnipresence of chirality in the world around us, especially in the living world. Several successful enantioselective CPL sensors and probes, mainly focused to biological targets, have been developed up to now.<sup>2d,8</sup> Going one step further, the possible practical implementation of a CPL-based microscopy would be a promising challenge in Biology.<sup>8f,g,9</sup> However, this interesting future technology still requires the development of both commercial CPL microscopes and batteries of efficient CPL dyes that can be used in biological media. In relation with the latter, the development of CPL laser dyes<sup>10</sup> enabling efficient, stable and tunable broad-line-width laser emission should be a top priority objective in CPL research, due to its potential application in different fields (*e.g.*, accurate study of biological processes involving chiral products,<sup>11</sup> efficient promotion of light-induced asymmetric processes,<sup>12</sup> or control of chiral morphologies in nanostructures<sup>13</sup>).

The level of CPL is quantified by the *luminescence dissymmetry factor*,  $g_{lum}$ , (see later), whose values stand between  $-2$  and  $+2$  (completely right and left polarized emission, respectively). Up to now, the highest levels of CPL have been mainly achieved from chiral lanthanide complexes,<sup>2d-e,8d-f</sup> which typically exhibit  $|g_{lum}|$  values within the  $0.05$ – $0.5$  range (an exceptional value of  $1.38$  has been reported for an europium(III) complex).<sup>14</sup> However, the emission efficiencies of these complexes are usually small, due to the nature of the involved metal-centered electronic transitions. This fact makes difficult their use in certain CPL applications (*e.g.*, in CPL lasing).

Some purely organic molecules afford CPL levels smaller than those obtained from the lanthanide complexes, when said molecules are hierarchically self-organized into nonracemic helical polymers or supramolecular aggregates ( $|g_{lum}|$  typically within the  $10^{-3}$ – $10^{-1}$  range).<sup>15</sup> Nonetheless, certain chirally super-organized polymeric cholesteric crystals (PCCs) can afford extraordinary levels of CPL. As an example, an impressive  $|g_{lum}|$  value of

ca. 1.6 has been reported for a light-emitting organic diode involving a three-layered PCC reflector.<sup>16</sup> Unfortunately, the hierarchical organization of the emissive system usually has a negative influence in the emission efficiency, especially when fluorescence is the emission phenomenon.

Nonetheless, organic molecules are highly valuable in photonics, mainly as a consequence of the next factors:

- High emission yields are possible.
- The emission can be modulated by accessible structural variations (a plethora of selective organic transformations on well-known organic chromophores is available).
- Valuable wide-band emission, allowing wavelength tunability.
- Easiness of specific manufacturing processes derived from the organic nature (*e.g.*, fabrication of ultrathin devices).

It is therefore obvious that the development of chiral organic molecules able to exhibit CPL efficiently, with both a large  $g_{lum}$  value and a high emission yield, is an interesting objective in the photonics field (to the best of our knowledge, there are no organic molecules with a fluorescence quantum yield larger than 88% that exhibit  $|g_{lum}|$  larger than  $3 \cdot 10^{-3}$ ). For approaching this objective, simple (small, nonpolymeric and nonaggregated) organic molecules enabling CPL (hereafter CPL-SOMs) are especially valuable due to three main factors: (1) good solubility in common organic solvents reducing fluorescence quenching by aggregation; (2) appropriate size for certain applications (*e.g.*, intracellular CPL bio-probing) or specific material manufacturing processes (*e.g.*, inclusion in solid matrixes); (3) absence of transition metals allowing applications where stability and/or environmental/toxicity factors are crucial. Unfortunately, CPL-SOMs are rare, and usually exhibit very small levels of CPL (typical  $|g_{lum}|$  values into the  $10^{-5}$ – $10^{-2}$  range), which has prompted a grown interest in the development of better CPL-SOMs, especially during the last five years, as shown below.

## CPL Measurement

### General Theory

The reader is referred to the numerous and extensive reviews that are devoted to CPL for a complete discussion of the CPL theory.<sup>2b,7b,c</sup> As such, only a brief overview of the theoretical principles is highlighted here. CPL spectroscopy allows one to measure the difference in the luminescence intensity ( $I$ ) of left circularly polarized light ( $I_L$ ) versus right circularly polarized light ( $I_R$ ). By convention this difference is defined as follows:

$$\Delta I \equiv I_L - I_R$$

Because of the difficulty in measuring absolute emission intensities, it is common to report the degree of CPL in terms of the luminescence dissymmetry factor (or ratio),  $g_{lum}$ , namely:

$$g_{lum} = \frac{\Delta I}{\frac{1}{2}I} = \frac{I_L - I_R}{\frac{1}{2}(I_L + I_R)}$$

which represents the ratio of the difference in intensity divided by the average total luminescence intensity. The extra factor of  $\frac{1}{2}$  in this equation is included to make the definition of  $g_{lum}$  consistent with the definition of the related quantity in CD, the *Kunh dissymmetry ratio*, namely,

$$g_{abs} = \frac{\Delta \varepsilon}{\varepsilon} = \frac{\varepsilon_L - \varepsilon_R}{\frac{1}{2}(\varepsilon_L + \varepsilon_R)}$$

Where  $\varepsilon$  has always been explicitly defined as an average quantity, and  $\varepsilon_L$  and  $\varepsilon_R$  indicate, respectively, the molar absorption coefficients for left and right circularly polarized light. Moreover, it was demonstrated that for the case of a randomly oriented emitting distribution the orientational averaging yields the following general result, where  $\mu^{gn}$  and  $m^{gn}$  refer to the electric dipole transition moment and the imaginary magnetic dipole transition moment.

$$g_{lum}(\lambda) = 4\text{Re} \left[ \frac{\mu^{gn} \cdot m^{gn}}{|\mu^{gn}|^2 + |m^{gn}|^2} \right]$$

One can expect the measurement of larger  $g_{lum}$  values when the transitions involved are inherently weak. This can be seen from the form of the latter equation, where one may expect a large  $g_{lum}$  value when the transition considered is electric dipole forbidden, but magnetic dipole allowed. Since the magnetic dipole transition moments are typically much smaller than the electric dipole terms, the denominator in the mentioned equation will be dominated by the first term,  $|\mu|^2$ . This is the reason for which CPL spectroscopy has been mainly applied to lanthanide(III) complexes, where large  $g_{lum}$  values can be reached for the magnetically-allowed intraconfigurational  $f-f$  transitions of the lanthanide ion.<sup>17</sup>

Unfortunately, the paradox of this requirement is that  $g_{lum}$  may be quite large (currently up to 1.38) for such selected transitions,<sup>14,18</sup> but they have usually very low intensity, and therefore are more difficult to measure. It is worth noting that the same arguments apply to CD spectroscopy, where it is often easier to study the  $n \rightarrow \pi^*$  transitions of chiral ketones than  $\pi \rightarrow \pi^*$  transitions. As a result, it is more challenging to apply CPL studies to chiral systems that are strongly luminescent, such as organic dyes, due to the presence of allowed transitions. That is the reason why chiral CPL-SOMs exhibit almost always  $|g_{lum}|$  values less than  $10^{-2}$ .

### Instrumentation and Measurement Artifacts

Although there is still a limited use of commercial CPL instruments, the technique has continued to be developed to a point where the detection of CPL can be performed with a high degree of sensitivity ( $\sim 1$  part in  $10^4$ – $10^5$ ) and reliability. It is worth noting that the

Author Manuscript

basic design of custom-made CPL spectrometers is most likely based on the technological approach used for Muller and co-workers (Figure 1).<sup>7b</sup> That is, the instrument is utilized in photon-counting detection with various technological approaches of gated-photon counting. The reader is referred to the reviews that are devoted to CPL for a complete discussion of the CPL instrumentation.<sup>2b,7b,c</sup> Typically, the choice of the excitation source is driven by the type of information one is interested in getting from a CPL measurement. In general, one uses a laser excitation when either high-intensity, or wavelength or polarization selectivity is required, but also if one is concerned with potential photochemical degradation upon long UV-light exposure.

Author Manuscript

It must be emphasized that it is important to minimize the sources of depolarization. As a result, no optical elements should be placed between the sample compartment and the photoelastic (or elasto-optic) modulator (PEM). Doing so ensures that no linearly polarized luminescence would be detected, since this latter is 10 to 100 times more intense than circularly polarized emitted light. Additional information is provided below. In addition to the use of a right-angle detection (90° excitation mode), it is recommended that the emitted light once it had passed through the PEM and the linear polarizer travels through an appropriate filter. This ensures that no scattered excitation or other stray light is detected by the thermoelectrically cooled photomultiplier tube (PMT). In addition, the polarization of the laser beam, when a laser excitation source is used, needs to be aligned along the direction of emission (laboratory *z* direction) in order to minimize any polarization in the *xy* plane for the reasons discussed thereafter.

Author Manuscript

Indeed, it has been recognized for a long time that the principal source of artifacts in the measurement of CPL is the linear polarization in the luminescent beam. This phenomenon originates from the passing of linearly polarized light through the very slightly birefringent PEM.<sup>2b,14,17–19</sup> Since the intensity of a linear polarization signal is much larger than of a true CPL signal, it may lead to signals of comparable magnitudes, even if the birefringence is usually small (< 5%). As an example, luminescence that is 10% linearly polarized may be converted by this effect to circular polarization of about 0.5%, which is often larger than the true CPL signal.

Author Manuscript

Although the presence of linear polarization in the luminescence beam may lead to difficulties in terms of measuring true CPL signals, it is possible to considerably limit and/or eliminate its effect, if any may be present in the luminescence beam. Thus, the study of short-lived fluorescent chiral organic species (*e.g.*, in CPL-SOMs) and/or metal-based compounds, crystals, glasses, rigid sol-gels, or solutions of very high viscosities of chiral molecules such as long-lived lanthanide(III)-based systems may require the use of specific experimental geometries to ensure that no linear polarization in the luminescence beam is detected. These types of systems are often defined by the so-called “frozen” case (this implies that the orientational distribution of the molecules is isotropic and, also, independent of the direction of emission detection).<sup>2b,7b,c</sup> Examples of such experimental approaches include the rotation of the PEM and the linear polarizer in a way that the birefringent axis of the PEM is parallel to the plane of polarization of the emitted light, or the use of combinations of excitation/emission geometries and linear polarizers that are positioned at the so-called “magic-angles”.<sup>20</sup> The key point is that the sample is isotropic in the plane

perpendicular to the direction of emission detection. This ensures that no linear polarization is detected in the (*xy*) plane. For example, this is the experimental approach used in the measurement of CPL from chiral triarylamine helicenes.<sup>21</sup> The excitation beam was linearly polarized along the laboratory *z* axis and, thus, resulting in the fact that no linear polarization was detected in the (*xy*) plane. Another example from the CPL study of chiral perylene-based aggregates, showed that these latter samples were excited at 0° in an epiluminescence measurement using a depolarized argon-ion laser excitation beam.<sup>22</sup> This, again, ensured that no linear polarization in the luminescence was detected. It should be emphasized that the most likely best way to ensure that no linear polarization is observed in the luminescence beam, or at least in the plane perpendicular to the emission detection, is by experiment. As it is the case for the conduct of routine standardization and calibration tests of CPL instrumentation, this is another important technical aspect of the measurements if one wants to report accurate CPL results.

Unlike CD spectroscopy, where all the absorbing chromophores contribute to the observed differential absorption measurement, CPL spectroscopy is limited to luminescent species. It must be emphasized that one needs to be careful on how to interpret CPL results with respect to the distribution of complex species present in solution. It is essential to know what the sample solution contains to avoid misinterpretation, since the CPL and total luminescence intensity from solutions of a mixture of optically active systems may come from different species.

### Calibration and Standards

Since the CPL technique is mainly based on a photon-counting method, it is possible to calculate the standard deviation,  $\sigma_d$ , in the measurement of the  $g_{lum}$  directly from the total number of photon counts, *N*.

$$\sigma_d = \sqrt{2/N}$$

This is possible since the function  $\sigma_d$  follows a Poisson distribution.<sup>23</sup> One can see that the determination of accurate  $g_{lum}$  for transitions associated with large  $g_{lum}$  values of highly luminescent systems can be done in a short time. On the other hand, a longer time of collection is necessary for transitions associated with small  $g_{lum}$  values of weakly luminescent species for achieving the same percentage error. As the time required for measuring a CPL spectrum is dependent on the intensity of the luminescence of the system of interest and the “chirality” of the transition analyzed, it is standard practice that the photon-pulses are collected for the same amount of time at each wavelength. Thus, the relative error (or signal-to-noise ratio) at each of these wavelengths is the same in the CPL spectrum measured.

Since there is a considerable increase in the use of CPL spectroscopy that mainly relies on homemade instruments, it is important to make sure that these apparatuses are regularly tested and calibrated to ensure the determination of accurate  $g_{lum}$  values. This is even more important for the accurate detection of small degrees of circular polarization in the total

emitted light intensity, which is typical for short-lived fluorescent chiral organic compounds like SOMs. It should be pointed out that this is a key step even for spectrometers that are based on an analog detection of CPL.<sup>2b,16</sup> The  $I$  and  $I$  data, which are proportional to the output of the lock-in amplifier and a DC output voltage, respectively, are typically acquired from two independent measurements. As a result, the determination of a  $g_{lum}$  necessitates the use of a calibration standard. On the other hand, the CPL instrumentation based on the photon counting method does not require the use of an independent calibration since, in this case, the  $g_{lum}$  is determined directly. However, it is always important to make sure that the magnitude and sign of the CPL signal are measured accurately.

Although various standardization and calibration methods have been utilized (*e.g.*, use of variable quarter-wave plates or passing unpolarized light through solutions of known CD),<sup>24,25</sup> the most popular approach consists in the use of a calibrant. The idea is that one measures the CPL activity of a solution containing a chiral species of known CPL.<sup>2b,16</sup> To date, the commercially available NMR chiral shift reagent tris(3-trifluoroacetyl-(+)-camphorato)europium(III), Eu((+)-facam)<sub>3</sub>, in DMSO is still the most used compound as a CPL standard.<sup>26</sup> Although this complex is available in high purity and can be excited either by a UV or argon-ion laser source, its use as a CPL calibration standard is still an area of argument and discussion.<sup>23,27</sup> The  $g_{lum}$  values of a DMSO solution of Eu((+)-facam)<sub>3</sub> at 588.2, 595.2, and 613.5 nm are -0.25, -0.78, and +0.072 in the spectral range of the <sup>5</sup>D<sub>0</sub>→<sup>7</sup>F<sub>1</sub> and <sup>5</sup>D<sub>0</sub>→<sup>7</sup>F<sub>2</sub> transitions, respectively. In addition to its water sensitivity, the high cost of Eu((-)-facam)<sub>3</sub> with the other enantiomeric form of facam limits its use as an effective and reliable CPL standard for routine tests. Working along these lines, Muller and co-workers have reported on the use of a more suitable CPL calibrating agent based on optical isomers of *N,N'*-bis(1-phenylethyl)-2,6-pyridinecarboxamide (BPEPC) coordinated to Eu(III) ions in a Eu:BPEPC ratio of 1:3 (Figure 2 and Table 1).<sup>28</sup> In particular, the advantages of these systems are: (1) the ease of the ligand synthesis, (2) their complex solution stability (*i.e.* several months), and (3) the lack of a noticeable photochemical degradation under continuous UV excitation (*i.e.*, 70 hours at 308 nm). We have tested that a  $g_{lum}$  value measured at 595.3 nm amounted to -0.18 for a [Eu((*R,R*)-(BPEPC))<sub>3</sub>]<sup>3+</sup> complex solution in MeCN left on the shelf and measured seven months apart.

Finally, it should be mentioned that the use of a calibrant to conduct instrumental routine tests also requires that one performs the necessary modifications to the apparatus in order to correct the source of the error and until the expected  $g_{lum}$  value is obtained. However, it is not appropriate to apply a factor of correction<sup>29</sup> to the experimental values of  $I$ ,  $I$ , or  $g_{lum}$  without some justification.<sup>7b,c</sup> This is not a suitable approach knowing that the accuracy and precision of CPL measurements are sample-specific, but also wavelength-dependent. In addition, each sample may respond differently to the various sources of error in CPL measurements (*e.g.*, electronic and optic elements). One may also encounter the presence of linear polarization in the emission, as already mentioned earlier.

### Early Reports on CPL-SOMs (1967–2007)

The first example of a CPL-SOM was (+)-(*S,S*)-trans- $\beta$ -hydrindanone ((*S,S*)-**1** in Figure 3), reported by Emeis and Oosterhoff in 1967.<sup>30</sup> This bicyclic chiral ketone was demonstrated

to show ultraviolet (UV) CPL by fluorescence in isooctane solution ( $g_{lum} = +3.5 \cdot 10^{-2}$  at 361 nm), upon exciting its carbonyl chromophore with UV light at 313 nm.<sup>30</sup> Note that the acting carbonyl chromophore is not chiral (inherently achiral), but its electronic transitions are *chirally perturbed* by the chiral structure where it is embedded.<sup>31</sup> From this first example, many other chiral ketones, mainly conformationally-restricted polycyclic ketones based on 2-norbornanone, such as (1*R*)-camphor ((**1R**)-**2**), (1*R*)-fenchone ((**1R**)-**3**), (1*R*)-camphenilone ((**1R**)-**4**) or (1*R*)-camphorquinone ((**1R**)-**5**) (Figure 3), have been reported to exhibit CPL by carbonyl fluorescence.<sup>32</sup> In all these cases, the maximal observed  $g_{lum}$  values were similarly small (typically within the  $10^{-3}$ – $10^{-2}$  range; see Table 2), the emissions taking place with low fluorescence quantum yields due to the nature of the involved carbonyl-centered transitions ( $n \rightarrow \pi^*$  and  $\pi^* \rightarrow n$ ).

Interestingly, Dekkers *and* co-workers early used the circularly polarized fluorescence of ketones as a spectroscopic tool to obtain information about the chiral structure of the emitting state. Thus, they discovered the possibility of specific carbonyl-ene bonding interactions in the emitting excited state of certain chiral polycyclic  $\beta,\gamma$ -enones (*e.g.*, (**1R**)-**6** and (**1S**)-**7** in Figure 4).<sup>32d</sup> In these cases, the described interaction of the acting carbonyl chromophore (dynamically coupled chromophore) causes an asymmetric distortion making it chiral (*inherently chiral*), but only at the emitting excited state. Significantly, these interesting early data on structures of emitting excited states were supported later by computational methods.<sup>33</sup>

Circularly polarized phosphorescence in simple chiral ketones was also early detected. Thus, Gafni and co-workers were able to measure the level of circularly polarized phosphorescence obtained from (**1R**)-**5** (Figure 3), by exciting the carbonyl chromophore in different solution conditions.<sup>32b</sup> Noticeably, the level of circular polarization was measured to be much smaller (by an order of magnitude) than the one reached by fluorescence in similar conditions, coming to demonstrate that the structures of the involved emitting states (triplet *vs.* singlet, respectively) are significantly different.

Obviously, fluorescent SOMs based on  $\pi$ -conjugated chromophores are more interesting for developing CPL materials than those based on single carbonyls, due to the possibility of higher fluorescent efficiencies coming from the  $\pi \rightarrow \pi^*$  (absorption) and  $\pi^* \rightarrow \pi$  (emission) transitions. To the best of our knowledge, the description of the UV circularly polarized fluorescence of  $C_2$ -symmetric calycanthine (**8** in Figure 5), reported by Barnett, Drake and Mason in 1979, constitutes the first example of a  $\pi$ -conjugated CPL-SOM ( $g_{lum} = +8 \cdot 10^{-3}$  upon UV excitation in ethanol).<sup>25</sup> As in the case of the chiral ketones, the aniline chromophore involved in the CPL activity of calycanthine is not chiral *per se*, but chirally perturbed by the chiral structure where it is embedded.

Extending the  $\pi$ -conjugation of the chromophore makes possible the generation of CPL in the visible (Vis) spectral region. Thus, Gossauer *and* co-workers early reported Vis circularly polarized fluorescence from the central  $\pi$ -extended difluoroboradipyromethene (BODIPY) chromophore of chiral (**R,R**)-**9** (Figure 5), upon exciting the urobilinoid (dihydropyrrolone) chromophores tethered to it (irradiation at 366 nm in  $\text{CH}_2\text{Cl}_2$ ;  $g_{lum}$  *ca.*  $+1 \cdot 10^{-3}$  at *ca.* 546 nm).<sup>34</sup> Therefore, an energy-transfer process is involved in the CPL



activity of **(R,R)-9**. Interestingly, a favored  $C_2$ -symmetric conformation involving intramolecular NH-F bonding was demonstrated to exist in **(R,R)-9**, which must favor the chiral perturbation of the emitting achiral BODIPY.<sup>34</sup> Noticeably, the photoluminescence efficiency of **(R,R)-9** was significantly high (48%), as expected from a highly-efficient BODIPY chromophore.

Helical chirality and extended  $\pi$ -conjugation make helicenes interesting chromophores for CPL. In 2001, Katz and co-workers described the polarization of the Vis fluorescence of [7]helicene-like **(M)-10** (Figure 6) at 440 nm, dissolved in dodecane ( $2 \cdot 10^{-6}$  M), upon irradiation at 325 nm (magnitude of the polarization ( $P$ ) *ca.*  $0.02 \pm 0.01$ ; 0.5 being the maximum possible).<sup>35</sup> Unfortunately, the extent to which this emission was circularly polarized was not reported but, interestingly, CPL was detected from aggregated species formed by increasing the concentration above  $1 \cdot 10^{-3}$  M.<sup>35</sup>

In 2003, Venkataraman and co-workers described the first detection of Vis circularly polarized fluorescence from nonaggregated helicenes (*e.g.*, **(1S,M)-11** and **(1S,M)-12** in Figure 6).<sup>21</sup> The basic helicene-like moiety of these compounds was firstly obtained as a racemic mixture and, then, resolved through derivatization to the diastereomeric (1S)-camphanates. Noticeably, the corresponding diastereomeric pairs for each helicene structure (*e.g.*, **(1S,M)-** and **(1S,P)-11**) exhibited enantiomerically-like complementary (oppositely signed) Vis CPL upon Vis irradiation in  $\text{CHCl}_3$  ( $|g_{lum}|$  *ca.*  $1 \cdot 10^{-3}$ , see Table 2), which demonstrates the lack of influence of the (1S)-camphanate moiety on the CPL activity of the acting inherently-chiral helicene chromophore.<sup>21</sup> Interestingly, **9-12** have two structural characteristics which are valuable for designing CPL-SOMs: (1) helicity and; (2) bulky functional groups avoiding the common fluorescence-quenching aggregation taking place in highly-extended  $\pi$ -conjugated systems.

Four years later, Kawai and co-workers described **13** (Figure 7) as the first CPL-SOM with a significantly high fluorescence quantum yield ( $\phi = 88\%$ ) in  $\text{CHCl}_3$ .<sup>36</sup> This molecule exemplifies a new structural design for CPL-SOMs, consisting in tethering two identical highly-extended achiral  $\pi$ -conjugated chromophores (in this case, the perylene-based diimides) to the ends of a central spacer with axial chirality (in this case, the atropisomeric 1,1'-binaphthyl moiety). **(R<sub>a</sub>)-** and **(S<sub>a</sub>)-13** were demonstrated to produce complementary Vis circularly polarized fluorescence ( $|g_{lum}|$  *ca.*  $3 \cdot 10^{-3}$  at *ca.* 550 nm; see Table 2), upon Vis irradiation (488 nm) in  $\text{CHCl}_3$  solutions (*ca.*  $10^{-7}$  M).<sup>22,36</sup> Increasing the concentration (above *ca.*  $10^{-4}$  M) was shown to improve the level of CPL ( $|g_{lum}|$  up to  $6 \cdot 10^{-3}$  at *ca.* 630 nm) due to self-organization by aggregation, but with an expected significant diminution of the fluorescence quantum yield (colloidal opaque solutions were obtained, and epillumination optics was required for measuring the CPL level).<sup>22</sup>

## Recent advances in CPL-SOMs (2011–2015, the blooming lustrum)

Chiral helicene has proved a valuable structural design for the development of CPL-SOMs. The group of Tanaka has successfully exploited this strategy since 2012,<sup>37</sup> synthesizing several enantioenriched [7]helicene-like CPL-SOMs through key enantioselective annulation reactions involving achiral alkyne precursors and chiral metal-complex catalysts.

For example, [7]helicene-like (**M**)-**14** and (**M**)-**15** (Figure 8) afforded very good levels of Vis circularly polarized fluorescence in  $\text{CHCl}_3$ , upon UV irradiation ( $g_{lum}$  ca.  $-3 \cdot 10^{-2}$ ).<sup>37a</sup>

Interestingly, Tanaka and co-workers have also reported enhanced CPL activity for S-shaped double azahelicenes when compared with parent single helicenes. As an example, upon UV irradiation in  $\text{CHCl}_3$ , S-shaped (**M,M**)-**16** (Figure 8) exhibits Vis circularly polarized fluorescence with  $g_{lum} = -1.1 \cdot 10^{-2}$  at 454 nm, whereas related (**M**)-**17** does it with  $|g_{lum}| < 1 \cdot 10^{-3}$  (measurable limit for the authors) at 467 nm.<sup>37b</sup> In 2012, Shinokubo and coworkers obtained aza[7]helicenes **18** (Figure 8) by oxidation of parent 2-aminoanthracene, followed by final chiral-HPLC resolution.<sup>38</sup> CPL-SOM (**M**)- and (**P**)-**18** exhibited complementary Vis circularly polarized fluorescence in  $\text{CH}_2\text{Cl}_2$  ( $|g_{lum}| = 3 \cdot 10^{-3}$ , see Table 2) upon irradiation at 375 nm.<sup>38</sup> Also following the [7]helicene strategy, Nozaki and co-workers have reported complementary Vis circularly polarized fluorescence from both enantiomers of sila[7]helicene **19** (Figure 8;  $|g_{lum}| = 3.5 \cdot 10^{-3}$ , upon UV irradiation in  $\text{CH}_2\text{Cl}_2$ ; see Table 2).<sup>39</sup> These CPL-SOMs were prepared by Pt-catalyzed double intramolecular hydroarylation of an achiral diyne precursor, followed by chiral-HPLC resolution of the obtained racemic mixture.<sup>39</sup>

In the same line, Muller and co-workers have recently described complementary Vis circularly polarized fluorescence from SOMs **20** and **21** ( $|g_{lum}| = \text{ca. } 1 \cdot 10^{-3}$  at ca. 430 nm, upon excitation at 357 nm in acetonitrile; see Table 2).<sup>40</sup> In this case, each pair of structurally related helicenic derivatives (e.g., (**P**)-**20** and (**P**)-**21** in Figure 8) were synthesized from the corresponding enantiopure 2,2,7,7'-tetrahydroxy-1,1'-binaphthyl (i.e., 7,7'-dihydroxyBINOL), which was firstly obtained as racemic mixture, and then resolved by the differential precipitation of the corresponding diastereomeric (*S*)-proline complexes.<sup>40</sup>

Unfortunately, the fluorescence quantum yields of the up-to-now reported helicene-like CPL-SOMs are moderate in the best of the cases (e.g., 32% for **14**, 36% for **18** or 23% for **19**, in the corresponding solution conditions; see Table 2), probably due to the distortion of the chromophore  $\pi$ -plane, which, on the other hand, is responsible of its chirality (inherent chirality) and chiroptical activity.

Obviously, using designs based on chirally-perturbed simple  $\pi$ -extended achiral chromophores (e.g., see **9** and **13**) seems to be the best option for obtaining CPL-SOMs with high emission efficiencies. In this line, de la Moya and co-workers have recently reported a new structural design for CPL-SOMs based on the use of achiral (nondistorted)  $\pi$ -extended chromophores.<sup>41</sup> The new design involves the straightforward use of a single  $C_2$ -symmetric chiral moiety for chirally perturbing the achiral chromophore. Moreover, to gain efficiency in the chiral perturbation, while the acting achiral chromophore remains electronically isolated, the perturbing chiral moiety is attached to the acting chromophore in an almost orthogonally-fixed arrangement. The new design was exemplified by the authors for CPL-SOM (**R<sub>a</sub>**)-**22** (Figure 9) and the corresponding enantiomer (**S<sub>a</sub>**)-**22**, which are based on BODIPY and BINOL, as the acting achiral  $\pi$ -extended chromophore and the chiral perturbing single moiety, respectively.<sup>41</sup>

**(R<sub>a</sub>)-** and **(S<sub>a</sub>)-22** exhibited complementary Vis circularly polarized fluorescence ( $|g_{lum}|$  ca.  $1 \cdot 10^{-3}$  at ca. 550 nm) with high fluorescent efficiency ( $\varphi = 46\%$ ), upon Vis-irradiation at 529 nm in CHCl<sub>3</sub> (see Table 2).<sup>41</sup>

Towards the same objective, Morisaki, Chujo and co-workers have developed interesting *D*<sub>2</sub>-symmetric [2.2]paracyclophane-based CPL-SOMs (e.g., **(S<sub>p</sub>)-23** and **(S<sub>p</sub>)-24** in Figure 9).<sup>42</sup> Noticeably, the propeller-shaped structure of **24** gives place to Vis circularly polarized fluorescence with very good both  $g_{lum}$  value and fluorescence quantum yield ( $g_{lum} = -1.1 \cdot 10^{-2}$  for **(S<sub>p</sub>)-24** at ca. 450 nm;  $\varphi = 45\%$ ), upon UV excitation at ca. 315 nm in CHCl<sub>3</sub> (see Table 2).<sup>42b</sup> Interestingly, the  $g_{lum}$  value exhibited by **(S<sub>p</sub>)-24** is ten-fold higher than that exhibited by its synthetic precursor **(S<sub>p</sub>)-23** ( $g_{lum} = +1.1 \cdot 10^{-3}$  at ca. 450 nm, upon exciting at 314 nm in the same solution conditions; see Table 2).<sup>42b</sup>

The good CPL behaviour of **24** results from its peculiar structure, which embeds an inherently-chiral (*D*<sub>2</sub>-symmetric) highly-extended criss-cross-delocalized chromophore.<sup>42</sup> Thus, although the plane of the involved  $\pi$ -conjugated chromophore is distorted (inherently chiral as it is the case for the helicenes), and should give place to low emission efficiencies, the [2.2]paracyclophane core allows an efficient through-space electronic interaction, giving place to electronic delocalization across the entire molecule (criss-cross delocalization).<sup>42a</sup> This additional electronic interaction must compensate the mentioned distortion, boosting the fluorescence efficiency. **(S<sub>p</sub>)-23** and **(S<sub>p</sub>)-24** (or **(R<sub>p</sub>)-23** and **(R<sub>p</sub>)-24**) were prepared from a key enantiopure planar-chiral [2.2]cyclophane intermediate, obtained firstly as a racemic mixture which was subsequently resolved ((1*S*)-camphanate-based diastereomers were formed, and elution chromatography used for the separation).<sup>42a</sup>

Establishing key structural factors controlling the level and sense of the CPL in closely related structures, as the just mentioned case for **(S<sub>p</sub>)-23** vs. **(S<sub>p</sub>)-24**, should be highly valuable for the future rational design of efficient CPL-SOMs. In this sense, the interesting studies conducted jointly by the groups of Fujiki and Imai, on the CPL behaviour of axially-chiral biaryl chromophores (e.g. **25-32** in Figure 10) must be highlighted.<sup>43</sup> Among other interesting findings, these authors have demonstrated that, for the same configuration of the chiral axe, the level and sense of the circularly polarized fluorescence of these compounds in CHCl<sub>3</sub> solution can be controlled by changing the biaryl dihedral angle (e.g., CPL reversal in **(S<sub>a</sub>)-25** vs. **(S<sub>a</sub>)-26**),<sup>43c</sup> the topology of the neighbouring groups (e.g., CPL-active **(R<sub>a</sub>)-27** vs. non-fluorescent **(R<sub>a</sub>)-28**),<sup>43e</sup> the linking aryl positions defining the chiral axe (e.g., CPL-active **(R<sub>a</sub>)-30** vs. CPL-silent **(R<sub>a</sub>)-31**)<sup>3h</sup> or the  $\pi$ -extension of the biaryl unit (CPL-silent **(R<sub>a</sub>)-31** vs. CPL-active **(R<sub>a</sub>)-32**; see Table 2).<sup>43h</sup> These biaryl-based CPL-SOMs typically exhibit UV circularly polarized fluorescence, upon UV-exciting the involved biaryl arenes, with  $|g_{lum}|$  values within the  $1.5 \cdot 10^{-3}$ – $0.8 \cdot 10^{-3}$  range at ca. the maximum emission wavelength (350–420 nm), and with fluorescent quantum yields standing typically within the ~15–25% range (see Table 2).<sup>43</sup>

Interestingly, Imai, Fujiki and co-workers have also demonstrated the possibility of Vis CPL from biaryls, by constructing proper excitation energy-transfer systems based on them, showing that **(R<sub>a</sub>)-29** (Figure 10) is able to act as a Vis-CPL-emitting energy-transfer

cassette, based on biaryl as the donor chromophore and anthracene as the acceptor ( $g_{lum} = +1 \cdot 10^{-3}$  at 422 nm; see Table 2).<sup>43e</sup>

The spatial arrangement of the acting chromophores plays a decisive role in controlling the sign of the CPL. Mori, Fujiki, Imai and co-workers have recently reported reversal circularly polarized fluorescence from (*S,S*)-**33** vs. (*S,S*)-**34** (Figure 11) in  $\text{CHCl}_3$  ( $g_{lum} = +9.4 \cdot 10^{-3}$  at 410 nm and  $-3.9 \cdot 10^{-3}$  at 375 nm, respectively), and correlated it with the spatial arrangement of the acting naphthalenes.<sup>44</sup> Unfortunately, the fluorescence quantum yield of these CPL-SOMs was very low (ca. 2%).<sup>44</sup> In the same research line, Nakashima, Kawai and co-workers have described that related (*S,S*)-**35** and (*S,S*)-**36** (Figure 11) exhibit Vis circularly polarized fluorescence with similar  $|g_{lum}|$  values (ca.  $6 \cdot 10^{-4}$  at ca. 540 nm), upon Vis irradiation (perylene excitation) in  $\text{CHCl}_3$ .<sup>45</sup> However, the sign of the corresponding  $g_{lum}$  values is opposite, negative for (*S,S*)-**35** and positive for (*S,S*)-**36** (see Table 2), which has been explained on the basis of the different major-conformations for both CPL-SOMs.<sup>45</sup> Noticeably, the fluorescent quantum yields of the latter CPL-SOMs were high (67% for (*S,S*)-**35** and 55% for (*S,S*)-**36**), due to the nature of the involved perylene-based chromophores.<sup>45</sup> It must be noted here that the design of the latter CPL-SOMs is the same used originally by Kawai and co-workers (see Figure 7),<sup>36</sup> consisting in arranging identical acting achiral chromophores at the ends of a central axially-chiral spacer.

Regarding the interest in controlling the CPL behaviour by structural factors, Abbate and co-workers have tried to rationalize the behaviour of four related [6]helicenes ((*P*)-**37-40** in Figure 12) in  $\text{CHCl}_3$ , by an interesting experimental and theoretical study based on DFT calculations. In all the cases, the sign of the CPL was related with the chiral configuration (negative for the (*P*) enantiomers), whereas the different substitution patterns cause a noticeable effect on the CPL magnitude, resulting higher for (*P*)-**37** and lower for (*P*)-**40** ( $g_{lum}$  values were not calculated), respectively.<sup>46</sup>

As highlighted in the introduction, CPL sensing is a promising field for CPL-SOMs. Regarding this issue, Maeda and coworkers have reported (*R<sub>a</sub>*)-**41** (Figure 13) as the first example of a chemical-stimuli-responsive CPL based on a SOM.<sup>47</sup> Thus, this CPL-silent molecule is able to produce a CPL signal under the presence of an excess of chloride anion in  $\text{CH}_2\text{Cl}_2$  solution ( $g_{lum} = -2 \cdot 10^{-3}$  at ca. 550 nm), upon irradiation at the isosbestic point of the absorption UV-Vis spectrum in  $\text{CH}_2\text{Cl}_2$ .<sup>47</sup> The obtained CPL signalization was attributed to a key conformational change in (*R<sub>a</sub>*)-**41**, caused by the anion binding.<sup>47</sup> Noticeably, the group of Maeda reported later that structures similar to **41**, but achiral, can produce similar CPL signalization by binding chiral anions (enantiomeric phenylalanine anions), which constitutes the first example of CPL bio-enantiosensing with a SOM.<sup>48</sup>

## General guidelines for the preparation of efficient CPL-SOMs

From the information summarized in Table 2, it is observed that helical designs, mainly based on helical chirality (helicene-like chromophores) or axial chirality (biaryls and multichromophore-decorated  $C_2$ -symmetric cores), have been extensively used for achieving CPL from SOMs in solution. These designs also allow higher fluorescence quantum yields (up to 88%) when compared to those based on chirally-perturbed ketones (up to  $1.7 \cdot 10^{-2}\%$ ).

Thus, using helicene-like chromophores have allowed to obtain the highest  $|g_{lum}|$  values (up to *ca.*  $3 \cdot 10^{-2}$ ) from a SOM. However, the preparation of these molecules is usually complex, requiring asymmetric catalysis and/or chiral resolution to obtain pure-enough enantiomers, which results in low overall yields. Moreover, the fluorescence quantum yields of the reported helicene-like SOMs are also usually low (up to 39%). On the other hand, SOMs based on biaryl chromophores have exhibited lower  $|g_{lum}|$  values (up to  $1.5 \cdot 10^{-3}$  in Table 2) than those observed for helicene-like SOMs, the fluorescence efficiencies being similar.

Higher fluorescence quantum yields than those exhibited by SOMs based on helicene-like and biaryl chromophores were measured for SOMs based on a multichromophore-decorated  $C_2$ -symmetric core (up to 88% in Table 2). Moreover, this structural design allows the preparation of CPL-SOMs, through straightforward synthetic routes in most of the cases, being possible to control the CPL sign, too. However, the highest  $g_{lum}$  values obtained to date from these multichromophoric SOMs were also associated to a noticeable loss of fluorescence efficiency (*e.g.*, see **(S,S)-33** in Table 2).

Beyond helicenes, biaryls and multichromophore-decorated  $C_2$ -symmetric cores, some other helical designs have been recently reported as interesting to enable CPL from SOMs. The aim of these new designs is to obtain high CPL values, keeping high fluorescence efficiencies. Among them, the elegant helical  $D_2$ -symmetric design of **24** must be highlighted, since it allows one of the highest  $g_{lum}$  values obtained to date from SOMs (up to  $1.3 \cdot 10^{-2}$ ), keeping a noticeably high fluorescence quantum yield (*ca.* 45%; see Table 2). However, its peculiar complex structure, based on a plane-chiral cyclophanic core, makes its preparation also complex from a synthetic point of view. Regarding this limit, the helical design of **22**, based on a highly fluorescent BODIPY chromophore, which is easy and efficiently perturbed by a chiral BINOL moiety, should result in an interesting starting point for the future development of CPL-SOMs, with both high  $g_{lum}$  values and high fluorescent efficiencies, through straightforward synthetic routes as well.

## Summary and outlook

As mentioned in the introduction, CPL-SOMs are rare, and the structural diversity of the involved chromophores, very poor, being practically restricted to carbonyls ( $\pi^* \rightarrow n$  transitions), and biaryls, helicenes, perylenes and BODIPYs ( $\pi^* \rightarrow \pi$  transitions). Moreover, the diversity of the structural designs for achieving the CPL phenomenon is very scarce yet, as shown above. On the other hand, the CPL levels reached up to now from SOMs are very small ( $|g_{lum}|$  up to  $3 \cdot 10^{-2}$ ), which makes difficult their practical application in the development of future CPL tools. Additionally, in many cases, the best CPL levels are not coincident with the best emission efficiencies, or with the easiest synthetic procedures. Despite all, the technological potential of the CPL-SOMs is huge (see Introduction), mainly due to the properties associated to their small size (which makes them interesting for the development of certain biological CPL applications beyond sensing), and their excellent organic-solvent solubility (which makes them valuable for the development of CPL-active dye-doped inclusion materials).

It is obvious that a further research aimed to the rational design and development of better CPL-SOMs, able to exhibit CPL with enough efficiency for practical applications (the current  $g_{lum}$  limit should be overcome), is required. However, this interesting objective is highly challenging due to the nature of the CPL phenomenon. Thus, it was shown that large CPL values are mainly obtained from electronic transitions with low probability, according to the normal selection rules. Nonetheless, it was also shown that the level and the sign of the CPL can be significantly affected by the degree of helical twist of the luminescent system, which opens a way for the future development of highly luminescent CPL-SOMs with emission of circularly polarized light greater than the current 0.3%.

## Acknowledgments

Spanish public funds from MINECO (Grants MAT2010-20646-C04-02 and MAT2014-51937-C3-2-P) of Spain and UCM (Grants GR3/14-910107 and -910150) are gratefully acknowledged. G.M. thanks the National Institutes of Health, Minority Biomedical Research Support (Grant 1 SC3 GM089589-05) and the Henry Dreyfus Teacher-Scholar Award for financial support. E.M.S.-C. thanks UCM for a predoctoral fellowship. Authors thank Gema de la Moya Cerero for the design of a frontispiece picture for this work.

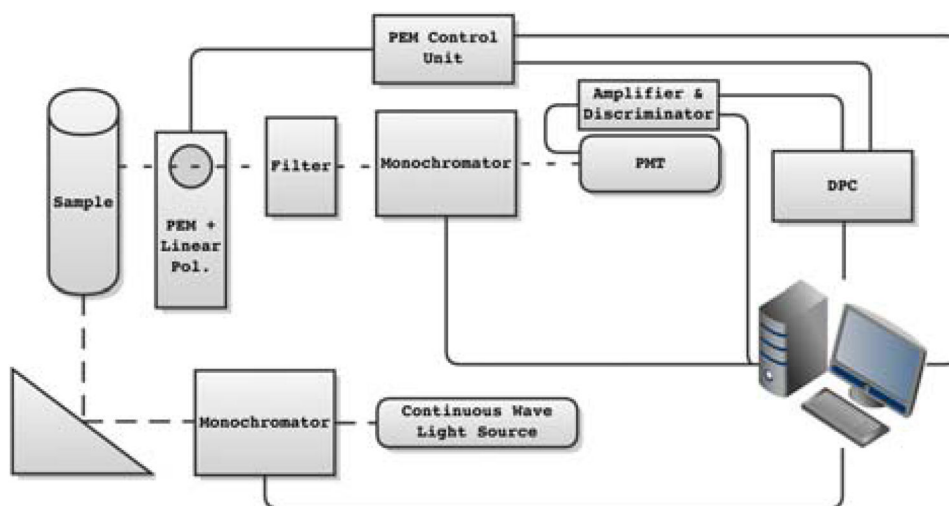
## References

1. a) Andrews, DL. Photonics, Vol. 1: Fundamental of Photonics and Physics. John Wiley and sons; Hoboken: 2015. b) Grynberg, G.; Aspect, A.; Fabre, C. Introduction to Quantum Optics: From the Semi-classical Approach to Quantized Light. Cambridge University Press; Cambridge: 2010. c) Latal, H. Chirality. From Weak Bosons to the  $\alpha$ -Helix. Janoschek, R., editor. Springer-Verlag; Berlin: 1991. p. 1-17.
2. a) Brittain HG. Chirality. 1996; 8:357–373. b) Riehl JP, Richardson FS. Chem Rev. 1986; 86:1–16. c) Berova, N.; Polavarapu, PL.; Nakanishi, K.; Woody, RW., editors. Comprehensive Chiroptical Spectroscopy Vol. 1. Instrumentation, Methodologies, and Theoretical Simulations. John Wiley and Sons; Hoboken: 2012. d) de Bettencourt-Dias, A., editor. Luminescence of Lanthanide ions in Coordination Compounds and Nanomaterials. John Wiley and Sons; Chichester: 2014. e) Zinna F, Di Bari L. Chirality. 2015; 27:1–13. [PubMed: 25318867]
3. Schadt M. Annu Rev Mater Sci. 1997; 27:305–379.
4. a) Wagenknecht C, Li CM, Reingruber A, Bao XH, Goebel A, Chen YA, Zhang Q, Chen K, Pan JW. Nat Photonics. 2010; 4:549–552. b) Sherson JF, Krauter H, Olsson RK, Julsgaard B, Hammerer K, Cirac I, Polzik ES. Nature. 2006; 443:557–560. [PubMed: 17024089]
5. Farshchi R, Ramsteiner M, Herfort J, Tahraoui A, Grahn HT. Appl Phys Lett. 2011; 98:162508, 3.
6. a) Jan CM. Opt Express. 2011; 19:5431–5441. [PubMed: 21445182] b) Yu CJ, Lin CE, Yu LP, Chou C. Appl Optics. 2009; 48:758–764.
7. a) Castiglioni E, Abbate S, Lebon F, Longhi G. Methods, Appl Fluoresc. 2014; 2:024006, 7. b) Muller, G. Luminescence of Lanthanide ions in Coordination Compounds and Nanomaterials. de Bettencourt-Dias, A., editor. John Wiley and Sons; Chichester: 2014. p. 77-124. c) Riehl, JP.; Muller, G. Comprehensive Chiroptical Spectroscopy Vol. 1. Instrumentation, Methodologies, and Theoretical Simulations. Berova, N.; Polavarapu, PL.; Nakanishi, K.; Woody, RW., editors. John Wiley and Sons; Hoboken: 2012. p. 65-90.
8. a) Saleh N, Moore B II, Srebo M, Vanthuyne N, Toupet L, Gareth Williams JA, Roussel C, Deol KK, Muller G, Autschbach J, Crassous J. Chem Eur J. 2015; 21:1673–1681. [PubMed: 25418503] b) Okutani K, Nozaki K, Iwamura M. Inorg Chem. 2014; 53:5527–5537. [PubMed: 24819655] c) Carr R, Puckrin R, McMahon BK, Pal R, Parker D, Pålsson LO. Methods Appl Floresc. 2014; 2:024007, 7. d) Heffern MC, Matosziuk LM, Meade TJ. Chem Rev. 2014; 114:4496–4539. [PubMed: 24328202] e) Carr R, Evans NH, Parker D. Chem Soc Rev. 2012; 41:7673–7686. [PubMed: 22895164] f) Muller G. Dalton Trans. 2009:9692–9707. [PubMed: 19885510] g) Seitz M, Moore EG, Ingram AJ, Muller G, Raymond KN. J Am Chem Soc. 2007; 129:15468–15470. [PubMed: 18031042]

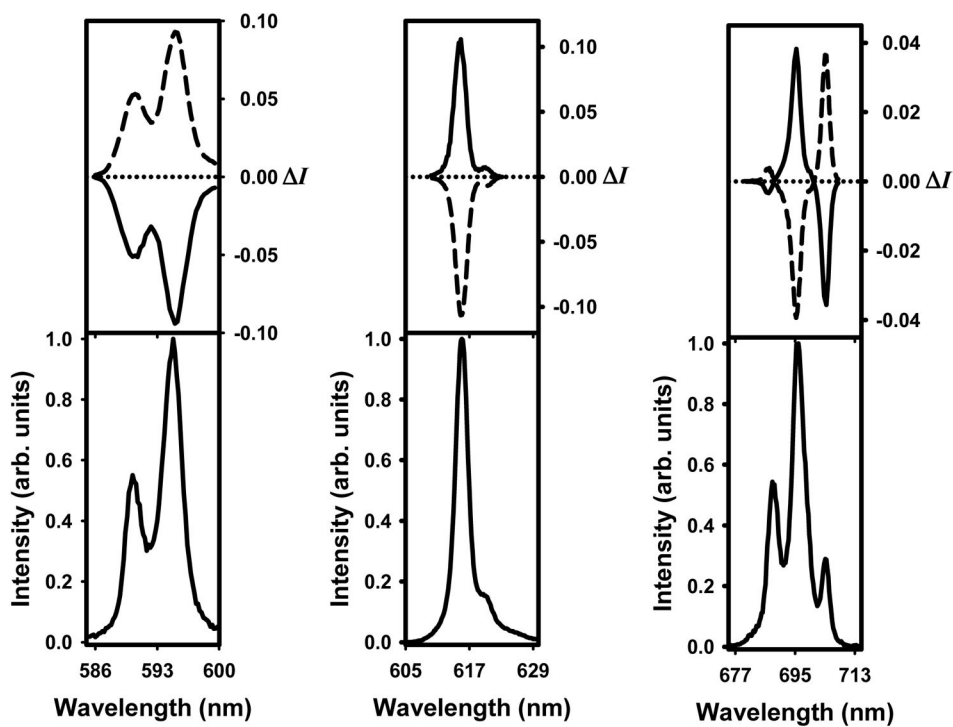
9. Tsumatori H, Harada T, Yuasa J, Hasegawa Y, Kawai T. *Appl Phys Express*. 2011; 4:011601, 3.
10. a) Topf RD, McCall MW. *Phys Rev A*. 2014; 90:053824, 5.b) Furumi S. *Chem Rec*. 2010; 10:394–408. [PubMed: 20954194]
11. a) Pavlov VA, Klabunovski EI. *Curr Org Chem*. 2014; 18:93–114.b) Jorissen A, Cerf C. *Orig Life Evol Biosph*. 2002; 32:129–142. [PubMed: 12185672]
12. a) Meinert C, Hoffmann SV, Cassam-Chenai P, Evans AC, Giri C, Nahon L, Meierhenrich UJ. *Angew Chem Int Ed*. 2014; 53:210–214.b) Cave RJ. *Science*. 2009; 323:1435–1436. [PubMed: 19286541] c) Pagni RM, Compton RN. *Mini-Rev Org Chem*. 2005; 2:203–209.
13. Yeom J, Yeom B, Chan H, Smith KW, Dominguez-Medina S, Bahng JH, Zhao G, Chang W-S, Chang S-J, Chuvilin A, Melnikau D, Rogach AL, Zhang P, Link S, Král P, Kotov NA. *Nature Mat*. 2015; 14:66–72.
14. Lunkley JL, Shirotani D, Yamanari K, Kaizaki S, Muller G. *J Am Chem Soc*. 2008; 130:13814–13815. [PubMed: 18816117]
15. a) Inouye M, Hayashi K, Yonenaga Y, Itou T, Fujimoto K, Uchida T, Iwamura M, Nozaki K. *Angew Chem Int Ed*. 2014; 53:14392–14396.b) Nagata Y, Takagi K, Suginone M. *J Am Chem Soc*. 2014; 136:9858–9861. [PubMed: 24941320] c) San Jose BA, Yan J, Akagi K. *Angew Chem Int Ed*. 2014; 53:10641–10644.d) Shiraki T, Tsuchiya Y, Noguchi T, Tamaru SI, Suzuki N, Taguchi M, Fujiki M, Shinkai S. *Chem Asian J*. 2014; 9:218–222. [PubMed: 24151104] e) Ng JCY, Liu J, Su H, Hong Y, Li H, Lam JWY, Wong KS, Tang BZ. *J Mat Chem C*. 2014; 2:78–83.f) Watanabe K, Suda K, Akagi K. *J Mat Chem C*. 2013; 1:2797–2795.g) Kumar J, Nakashima T, Tsumatori H, Kawai T. *Phys Chem Lett*. 2013; 5:316–321.h) Yang Y, Correa da Costa R, Smilgies D-M, Campbell A-J, Fuchter MJ. *Adv Mater*. 2013; 25:2624–2628. [PubMed: 23554220]
16. Jeong SM, Ohtsuka Y, Ha NY, Takanishi Y, Ishikawa K, Takezoe H, Nichimura S, Suzuki G. *Appl Phys Lett*. 2007; 90:211106, 3.
17. a) Richardson FS. *Inorg Chem*. 1980; 19:2806–2812.b) Luk CK, Richardson FS. *J Am Chem Soc*. 1975; 97:6666–6675.
18. Lunkley JL, Shirotani D, Yamanari K, Kaizaki S, Muller G. *Inorg Chem*. 2011; 50:12724–12732. [PubMed: 22074461]
19. Dekkers HPJM, Moraal PF, Timper JM, Riehl JP. *Appl Spectrosc*. 1985; 39:818–821.
20. Tinoco JJ, Ehrenberg B, Steinberg IZ. *J Chem Phys*. 1977; 66:916–920.
21. Field JE, Muller G, Riehl JP, Venkataraman D. *J Am Chem Soc*. 2003; 125:11808–11809. [PubMed: 14505389]
22. Tsumatori H, Nakashima T, Kawai T. *Org Lett*. 2010; 12:2362–2365. [PubMed: 20405955]
23. Schippers, PH. PhD Dissertation. University of Leiden; The Netherlands: 1982.
24. Steinberg IZ, Gafni A. *Rev Sci Instrum*. 1972; 43:409–413.
25. Barnett CJ, Drake AF, Mason SF. *Bull Soc Chim Belg*. 1979; 88:853–862.
26. Brittain HG, Richardson FS. *J Am Chem Soc*. 1976; 98:5858–5863.
27. Maupin, CL. PhD Dissertation. Michigan Technological University; 1999.
28. a) Bonsall SD, Houcheime M, Straus DA, Muller G. *Chem Commun*. 2007; 35:3676–3678.b) Hua KT, Xu J, Quiroz EE, Lopez S, Ingram AJ, Johnson VA, Tisch AR, de Bettencourt-Dias A, Straus DA, Muller G. *Inorg Chem*. 2012; 51:647–660. [PubMed: 22148725]
29. a) Coughlin FJ, Westrol MS, Oyler KD, Byrne N, Krami C, Zysman-Colman E, Lowry MS, Bernhard S. *Inorg Chem*. 2008; 47:2039–2048. [PubMed: 18271527] b) Matsumoto K, Suzuki K, Tsukuda T, Tsubomura TA. *Inorg Chem*. 2010; 49:4717–4719. [PubMed: 20438091]
30. Emeis CA, Oosterhoff LJ. *Chem Phys Lett*. 1967; 1:129–132.
31. a) Eliel, EL.; Wilen, SH.; Mander, LN. *Stereochemistry of Organic Compounds*. John Wiley and Sons; New York: 1994. b) Nógrádi, M. *Stereochemistry. Basic Concepts and Applications*. Pergamon Press; Oxford: 1981.
32. a) Dekkers HPJM, Closs LE. *J Am Chem Soc*. 1976; 98:2210–2219.b) Steinberg N, Gafni A, Steinberg IZ. *J Am Chem Soc*. 1981; 103:1636–1640.c) Schippers PH, Deckers HPJM. *J Am Chem Soc*. 1983; 105:145–146.d) Schippers PH, van der Ploeg JPM, Dekkers HPJM. *J Am Chem Soc*. 1983; 105:84–89.

33. a) Pecul M, Ruud K. *Phys Chem Chem Phys*. 2011; 13:643–650. [PubMed: 21031208] b) Longhi G, Castiglioni E, Abbate S, Lebon F, Lightner DA. *Chirality*. 2013; 25:589–599. [PubMed: 23840012]
34. Gossauer A, Fehr F, Nydegger F, Stöckli-Evans H. *J Am Chem Soc*. 1997; 119:1599–1608.
35. Phillips KES, Katz TJ, Jockusch S, Lovinger AJ, Turro NJ. *J Am Chem Soc*. 2001; 123:11899–11907. [PubMed: 11724596]
36. Kawai T, Kawamura K, Tsumatori H, Ishikawa M, Naito M, Fujiki M, Nakashima T. *Chem Phys Chem*. 2007; 8:1465–1468. [PubMed: 17557371]
37. a) Sawada Y, Furumi S, Takai A, Takeuchi M, Noguchi K, Tanaka K. *J Am Chem Soc*. 2012; 134:4080–4083. [PubMed: 22335235] b) Nakamura K, Furumi S, Takeuchi M, Shibuya T, Tanaka K. *J Am Chem Soc*. 2014; 136:5555–5558. [PubMed: 24670158]
38. Goto K, Yamaguchi R, Hiroto S, Ueno H, Kawai T, Shinokubo H. *Angew Chem Int Ed*. 2012; 51:10333–10336.
39. Oyama H, Nakano K, Harada T, Kuroda R, Naito M, Nobusawa K, Nozaki K. *Org Lett*. 2013; 15:2104–2107. [PubMed: 23587064]
40. Shyam Sundar M, Talele HR, Mande HM, Bedekar AV, Tovar RC, Muller G. *Tetrahedron Lett*. 2014; 55:1760–1764. [PubMed: 24707063]
41. Sánchez-Carnerero EM, Moreno F, Maroto BL, Agarrabeitia AR, Ortiz MJ, Vo BG, Muller G, de la Moya S. *J Am Chem Soc*. 2014; 136:3346–3349. [PubMed: 24524257]
42. a) Morisaki Y, Gon M, Sasamori T, Tokitoh N, Chujo Y. *J Am Chem Soc*. 2014; 136:3350–3353. [PubMed: 24527728] b) Gon M, Morisaki Y, Chujo Y. *J Mat Chem C*. 2015; 3:521–523.
43. a) Kinuta T, Sato T, Nakano Y, Harada T, Tajima N, Fujiki M, Kuroda R, Matsubara Y, Imai Y. *Photochem Photobiol, A: Chem*. 2011; 220:134–138. b) Kinuta T, Tajima N, Fujiki M, Miyazawa M, Imai Y. *Tetrahedron*. 2012; 68:4791–4796. c) Kimoto T, Tajima N, Fujiki M, Imai Y. *Chem Asian J*. 2012; 7:2836–2841. [PubMed: 23038101] d) Amako T, Kimoto T, Tajima N, Fujiki M, Imai Y. *RSC Adv*. 2013; 3:6939–6944. e) Amako T, Kimoto T, Tajima N, Fujiki M, Imai Y. *Tetrahedron*. 2013; 69:2753–2757. f) Amako T, Harada T, Suzuki N, Mishima K, Fujiki M, Imai Y. *RSC Adv*. 2013; 3:23508–23513. g) Nakabayashi K, Amako T, Tajima N, Fujiki M, Imai Y. *Chem Commun*. 2014; 50:13228–13230. h) Kitayama Y, Amako T, Suzuki N, Fujiki M, Imai Y. *Org Biomol Chem*. 2014; 12:4342–4346. [PubMed: 24789695] i) Kitayama Y, Nakabayashi K, Wakabayashi T, Tajima N, Fujiki M, Imai Y. *RSC Adv*. 2015; 5:410–415.
44. Amako T, Nakabayashi K, Mori T, Inoue Y, Fujiki M, Imai Y. *Chem Commun*. 2014; 50:12836–12839.
45. Kumar J, Nakashima T, Tsumatori H, Mori M, Naito M, Kawai T. *Chem Eur J*. 2013; 19:14090–14097. [PubMed: 24026812]
46. Abbate S, Longhi G, Lebon F, Castiglione E, Superchi S, Pisani L, Fontana F, Torricelli F, Corona T, Villani C, Sabia R, Tommasini M, Lucotti A, Mendola D, Mele A, Lightner DA. *J Phys Chem C*. 2014; 118:1682–1695.
47. Maeda H, Bando Y, Shimomura K, Yamada I, Naito M, Nobusawa K, Tsumatori H, Kawai T. *J Am Chem Soc*. 2011; 133:9266–9269. [PubMed: 21599014]
48. Maeda H, Shirai T, Bando Y, Takaishi K, Uchiyama M, Muranaka A, Kawai T, Naito M. *Org Lett*. 2013; 15:6006–6009. [PubMed: 24245585]

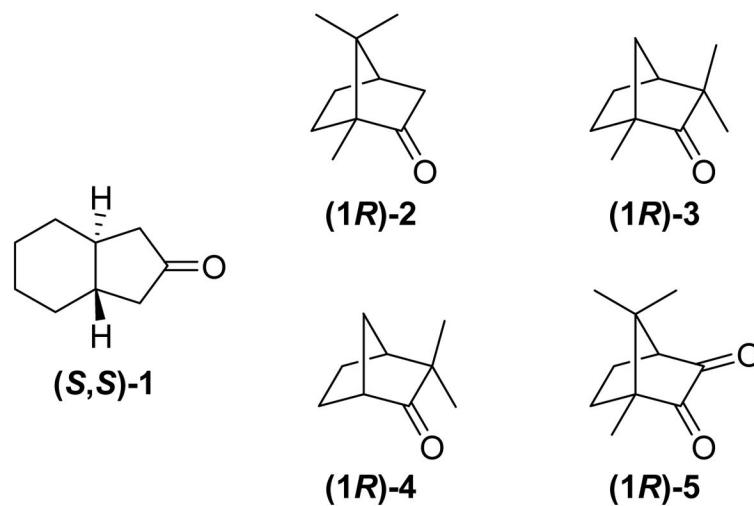




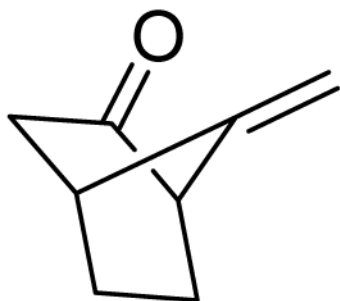
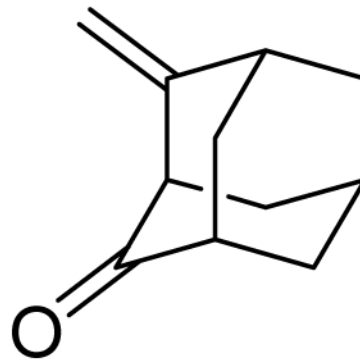
**Figure 1.** Schematic diagram for instrumentation used to perform CPL measurements.



**Figure 2.** CPL (upper curves) and total luminescence (lower curves) spectra for the  ${}^5D_0 \rightarrow {}^7F_1$  (left),  ${}^5D_0 \rightarrow {}^7F_2$  (middle), and  ${}^5D_0 \rightarrow {}^7F_3$  (right) transitions of the MeCN solutions ( $6.67 \cdot 10^{-3}$  M) of  $[\text{Eu}((R,R)\text{-BPEPC})_3]^{3+}$  (solid lines) and  $[\text{Eu}((S,S)\text{-BPEPC})_3]^{3+}$  (dashed lines) at 295 K, following excitation at 308 nm (see ref. 28a).



**Figure 3.**  
Some CPL-SOMs based on chirally-perturbed carbonyl chromophore.

**(1R)-6****(1S)-7**

**Figure 4.** Examples of CPL-SOMs based on dynamically-coupled chirally-perturbed carbonyl chromophore.

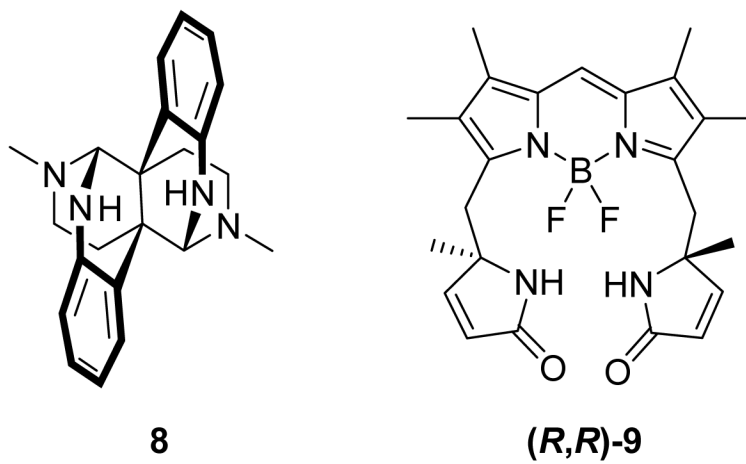


**Figure 5.**  
First CPL-SOMs based on chirally-perturbed  $\pi$ -conjugated chromophore.

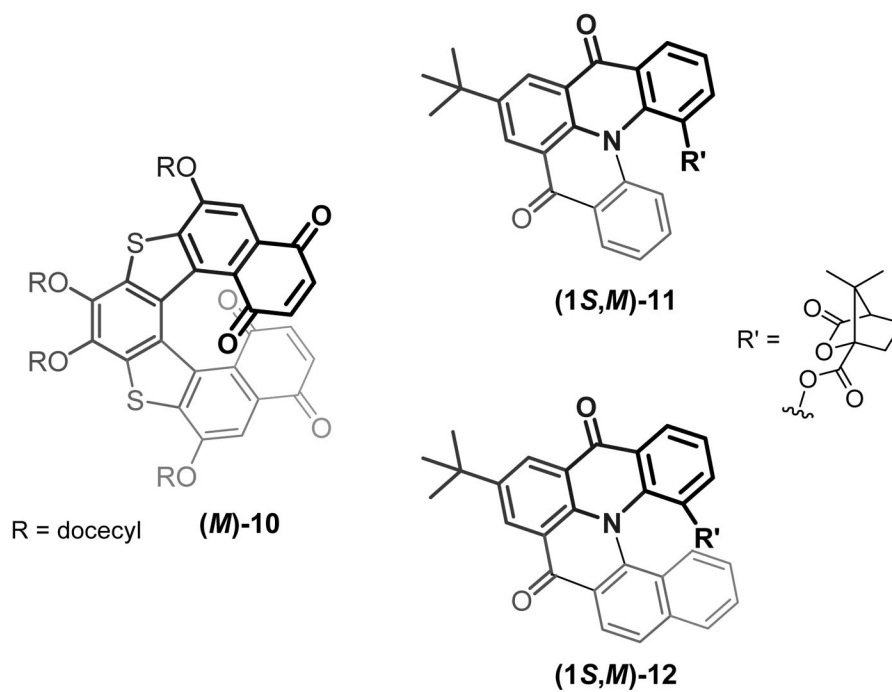


**Figure 6.**  
First Vis CPL-SOMs based on inherently-chiral helicene-like chromophore.

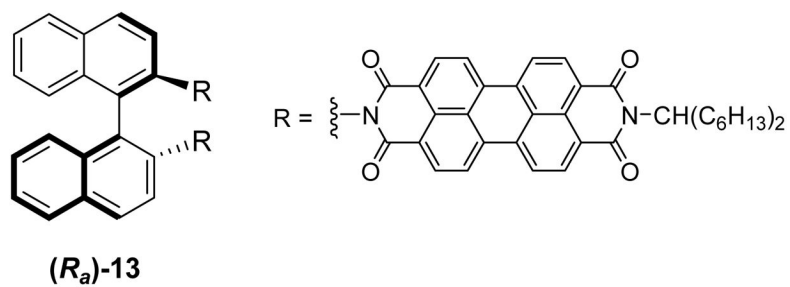


**Figure 7.** First CPL-SOMs based on two achiral chromophores attached to the ends of a central axially-chiral spacer.

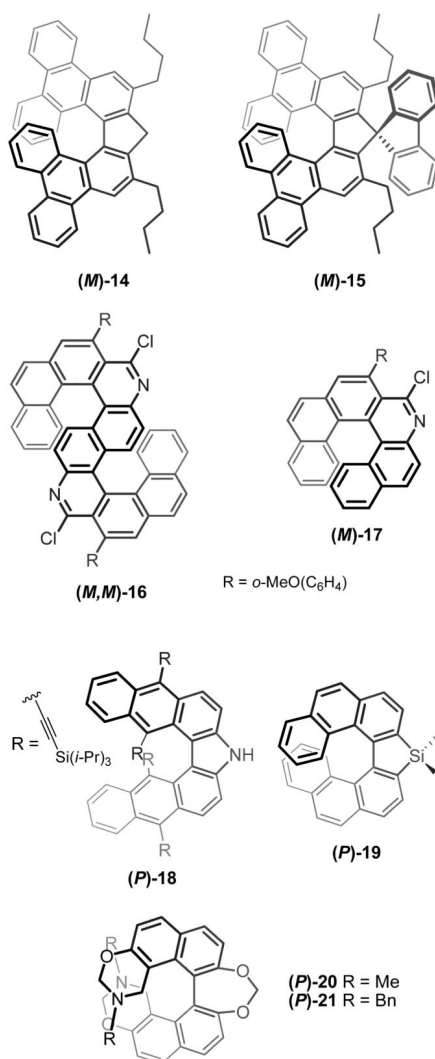


**Figure 8.**  
More CPL-SOMs based on inherently-chiral [7]helicenes.



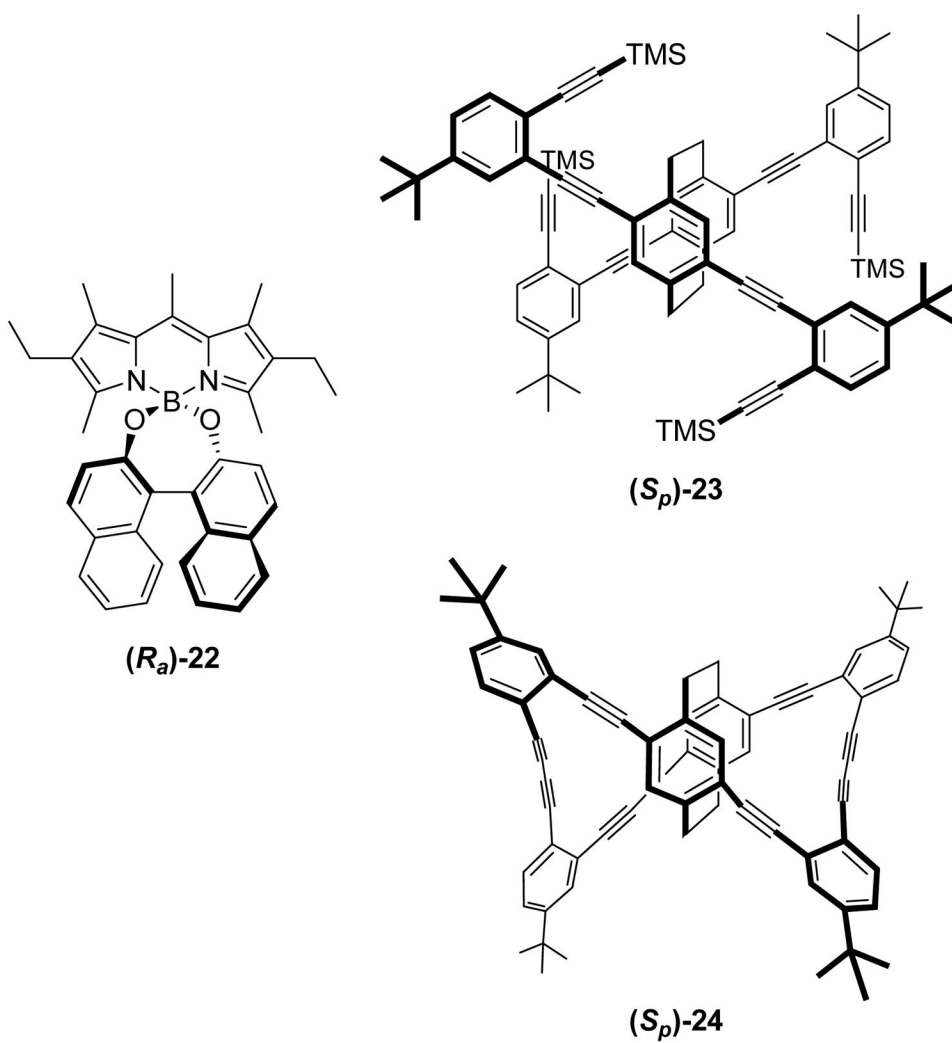


**Figure 9.**  
Recent designs for CPL-SOMs.

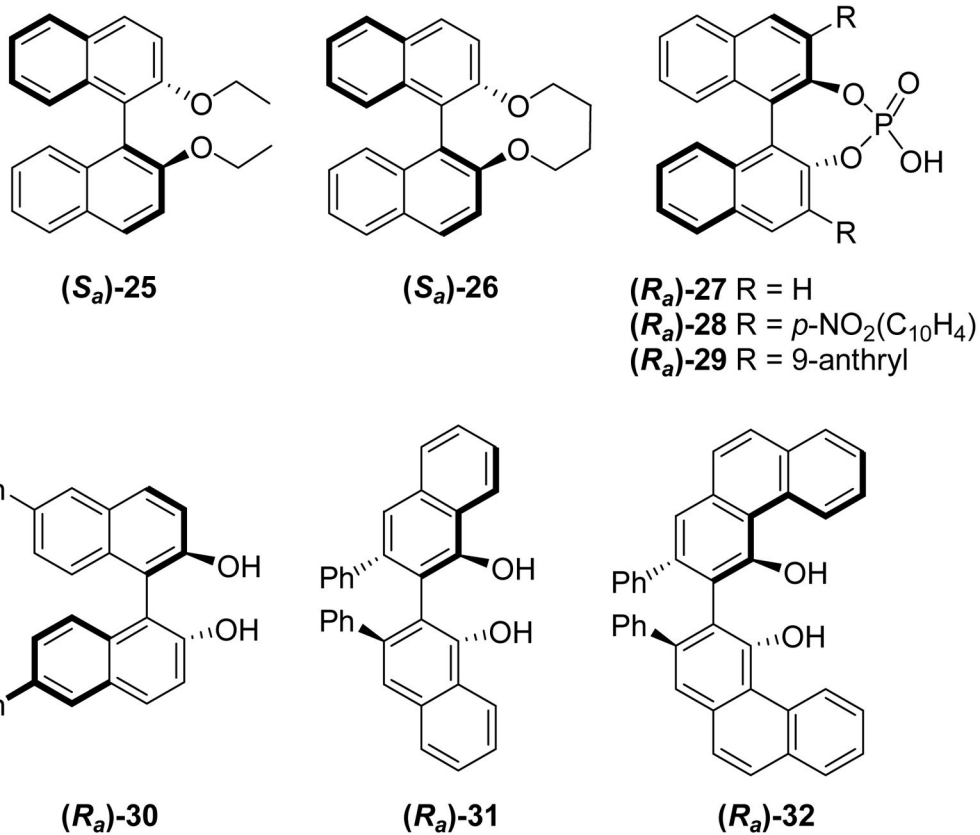


**Figure 10.** Some structural variations affecting CPL in biaryl-based CPL-SOMs.

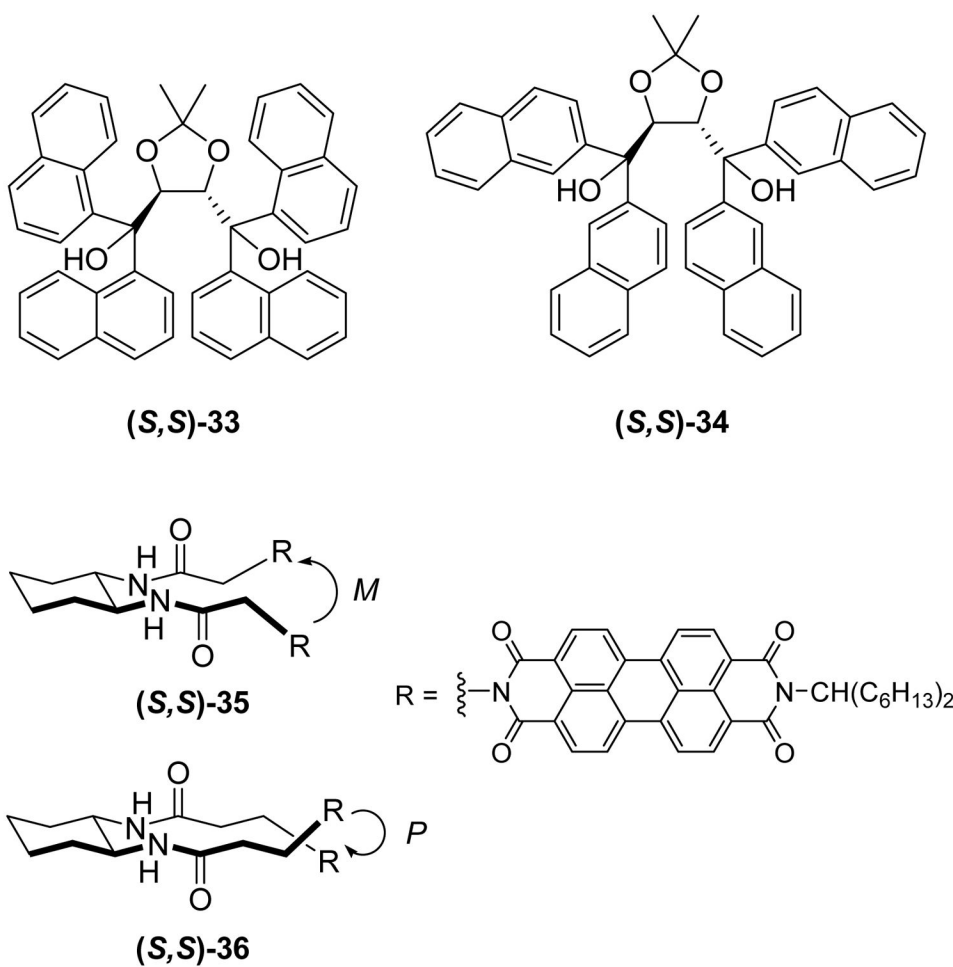


**Figure 11.** Some additional structural variations affecting the sign of the CPL in CPL-SOMs.

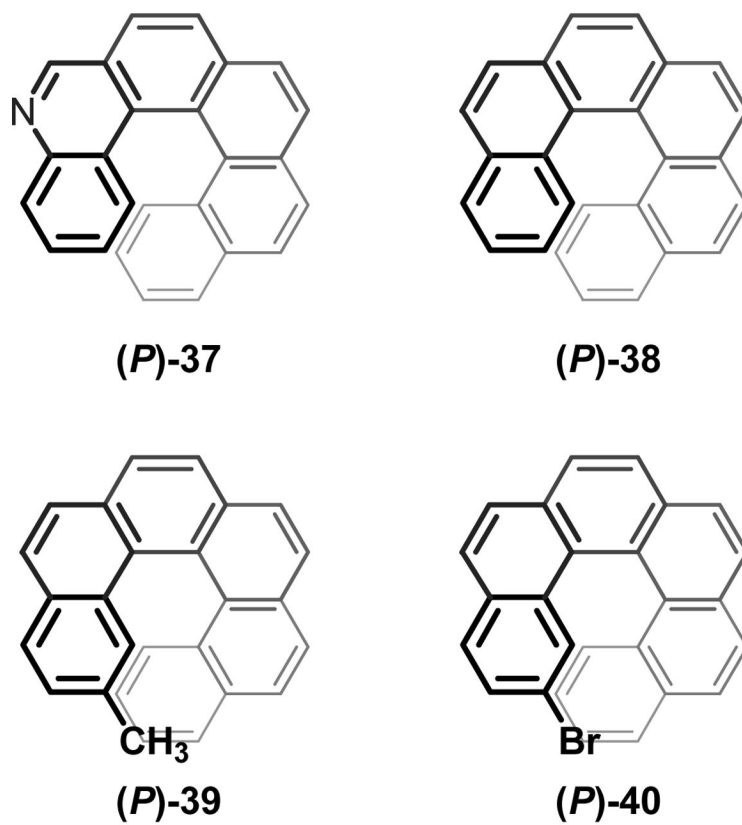


**Figure 12.**  
Some structural variations affecting the CPL magnitude in helicenes.

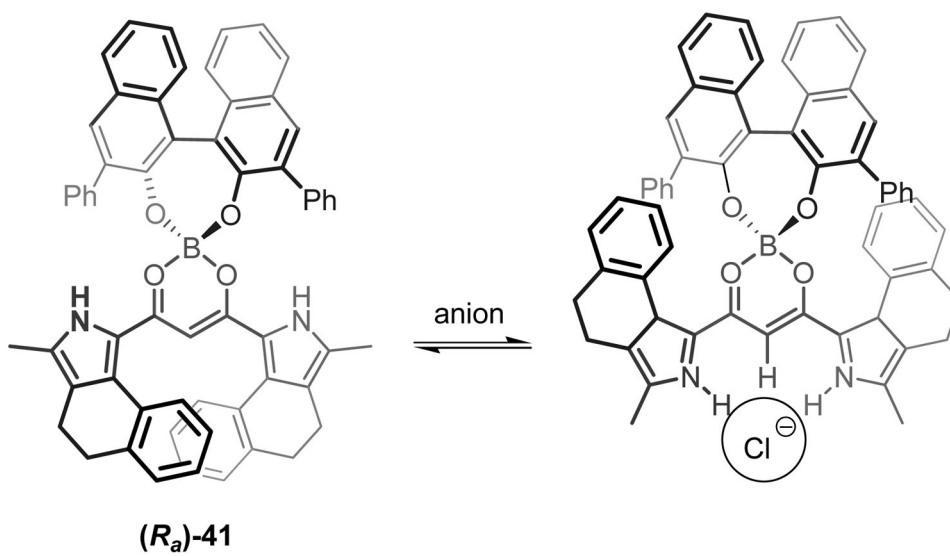


**Figure 13.**  
First example of chemical-stimuli-responsive CPL based on a SOM.

**Table 1**

Summary of CPL results for the MeCN solution ( $6.67 \cdot 10^{-3}$  M) of  $[\text{Eu}((R,R)\text{-BPEPC})_3]^{3+}$  at 295 K, following an excitation at 308 nm (see ref. 28a).

Electronic transition	Wavelength (nm)	$g_{lum} \pm 0.01$
$^5\text{D}_0 \rightarrow ^7\text{F}_1$	590.5/595.3	-0.19/-0.18
$^5\text{D}_0 \rightarrow ^7\text{F}_2$	615.6	+0.21
$^5\text{D}_0 \rightarrow ^7\text{F}_3$ [a]	649.6	-0.22
$^5\text{D}_0 \rightarrow ^7\text{F}_4$	688.8/696.0/704.1	+0.001/+0.07/-0.24

[a] Very low luminescence that prevents to record a complete CPL spectrum.

Table 2

Selected CPL-SOMs organized by designs, with their corresponding fluorescence quantum yield ( $\phi_f$ ), as well as CPL data (solvent, concentration, excitation wavelength and  $g_{lum}$  values). The higher fluorescence efficiencies and CPL behaviours within a design family have been underlined.

Chromophore design	CPL-SOM	$\phi_f/\%$	CPL data		Ref.	
			solvent (concentration/M)	$\lambda_{exc}/nm$ $g_{lum}$ ( $\lambda/nm$ )		
Chirally perturbed ketone	( <i>S,S</i> )- <b>1</b>	<i>ca.</i> $1 \cdot 10^{-3}$	isooctane ( $5 \cdot 10^{-2}$ )	313	<u><math>\pm 3.5 \cdot 10^{-2}</math></u> (361)	30,32c
	( <i>R</i> )- <b>2</b>	n.a.	EtOH ( $2 \cdot 10^{-2}$ )	290	<i>ca.</i> $-4 \cdot 10^{-3}$ ( <i>ca.</i> 450)	33b
	( <i>R</i> )- <b>5</b>	n.a.	TFE/ <i>dl</i> -MeOH 1:1 ( $1 \cdot 10^{-2}$ )	440	<i>ca.</i> $-1 \cdot 10^{-2}$ (550)	32b
	( <i>R</i> )- <b>6</b>	$6 \cdot 10^{-3}$	heptane ( $5 \cdot 10^{-3}$ )	300	<u><math>+15.7 \cdot 10^{-3}</math></u> ( <i>ca.</i> 400)	32d
	( <i>S</i> )- <b>7</b>	<u><math>1.7 \cdot 10^{-2}</math></u>	heptane ( $5 \cdot 10^{-3}$ )	290	$-6.3 \cdot 10^{-3}$ ( <i>ca.</i> 400)	32d
	( <i>S,M</i> )- <b>11</b>	n.a.	CHCl <sub>3</sub> (n.a.)	n.a.	$-1.1 \cdot 10^{-3}$ (453)	21
	( <i>S,P</i> )- <b>11</b>	n.a.	CHCl <sub>3</sub> (n.a.)	n.a.	<u><math>+0.9 \cdot 10^{-3}</math></u> (453)	21
Helicene-like	( <i>S,M</i> )- <b>12</b>	n.a.	CHCl <sub>3</sub> (n.a.)	n.a.	$-0.7 \cdot 10^{-3}$ (478)	21
	( <i>S,P</i> )- <b>12</b>	n.a.	CHCl <sub>3</sub> (n.a.)	n.a.	<u><math>+0.8 \cdot 10^{-3}</math></u> (478)	21
	( <i>M</i> )- <b>14</b>	32	CHCl <sub>3</sub> ( $2 \cdot 10^{-5}$ )	375	$-3.0 \cdot 10^{-2}$ (428)	37a
	( <i>M</i> )- <b>15</b>	30	CHCl <sub>3</sub> ( $2 \cdot 10^{-5}$ )	375	<u><math>-3.2 \cdot 10^{-2}</math></u> (449)	37a
	( <i>M,M</i> )- <b>16</b>	0.94	CHCl <sub>3</sub> ( $1 \cdot 10^{-6}$ )	375	$-1.1 \cdot 10^{-2}$ (454)	37b
	( <i>M</i> )- <b>17</b>	0.21	CHCl <sub>3</sub> (n.a.)	375	$< \pm 1 \cdot 10^{-3}$	37b
	( <i>P</i> )- <b>18</b>	<u>36</u>	CH <sub>2</sub> Cl <sub>2</sub> (n.a.)	375	<u><math>+3 \cdot 10^{-3}</math></u> ( <i>ca.</i> 550)	38
	( <i>M</i> )- <b>18</b>	n.a.	CH <sub>2</sub> Cl <sub>2</sub> (n.a.)	375	$-3 \cdot 10^{-3}$ ( <i>ca.</i> 550)	38
	( <i>P</i> )- <b>19</b>	23	CH <sub>2</sub> Cl <sub>2</sub> ( $6.8 \cdot 10^{-6}$ )	n.a.	$+3.5 \cdot 10^{-3}$ (470)	39
	( <i>P</i> )- <b>20</b>	n.a.	MeCN ( $1 \cdot 10^{-3}$ )	357	<u><math>+1.5 \cdot 10^{-3}</math></u> ( <i>ca.</i> 430)	40
Biaryl	( <i>M</i> )- <b>20</b>	n.a.	MeCN ( $1 \cdot 10^{-3}$ )	357	$-0.9 \cdot 10^{-3}$ ( <i>ca.</i> 430)	40
	( <i>P</i> )- <b>21</b>	n.a.	MeCN ( $1 \cdot 10^{-3}$ )	357	<u><math>+1.4 \cdot 10^{-3}</math></u> ( <i>ca.</i> 430)	40
	( <i>M</i> )- <b>21</b>	n.a.	MeCN ( $1 \cdot 10^{-3}$ )	357	$-1.3 \cdot 10^{-3}$ ( <i>ca.</i> 430)	40
	( <i>S<sub>a</sub></i> )- <b>25</b>	19	CHCl <sub>3</sub> ( $1 \cdot 10^{-3}$ )	330	<u><math>+1 \cdot 10^{-3}</math></u> ( <i>ca.</i> 370)	43c
	( <i>S<sub>a</sub></i> )- <b>26</b>	25	CHCl <sub>3</sub> ( $1 \cdot 10^{-3}$ )	330	$-1.4 \cdot 10^{-3}$ ( <i>ca.</i> 370)	43c
	( <i>R<sub>0</sub></i> )- <b>27</b>	29	CHCl <sub>3</sub> ( $1 \times 10^{-5}$ )	302	<u><math>+1.5 \cdot 10^{-3}</math></u> ( <i>ca.</i> 350)	43a-b

Chromophore design	CPL-SOM	$\phi_p$ /%	CPL date solvent (concentration/M)	$\lambda_{exc.}/nm$	$g_{lum}$ ( $\lambda/nm$ )	Ref.
	( <i>R<sub>p</sub></i> )-29	39	CHCl <sub>3</sub> (1·10 <sup>-4</sup> )	350	+1·10 <sup>-3</sup> (ca. 420)	43e
	( <i>R<sub>p</sub></i> )-30	0.5	CHCl <sub>3</sub> (1·10 <sup>-4</sup> )	320	ca. -7.8·10 <sup>-4</sup> (ca. 373)	43h
	( <i>R<sub>p</sub></i> )-31	n.a.	CHCl <sub>3</sub> (n.a.)	n.a.	Silent	43h
	( <i>R<sub>p</sub></i> )-32	20	CHCl <sub>3</sub> (1·10 <sup>-5</sup> )	282	-1.3·10 <sup>-3</sup> (ca. 380)	43h
<hr/>						
Multichromophore-decorated C <sub>2</sub> -symmetric core						
	( <i>R<sub>p</sub></i> )-13	88	CHCl <sub>3</sub> (5.6·10 <sup>-7</sup> )	488	ca. -3·10 <sup>-3</sup> (ca. 555)	22
	( <i>S<sub>d</sub></i> )-13				ca. +3·10 <sup>-3</sup> (ca. 555)	
	( <i>S<sub>s</sub></i> )-33	2	CHCl <sub>3</sub> (1·10 <sup>-3</sup> )	290	ca. +9.4·10 <sup>-3</sup> (410)	44
	( <i>R<sub>r</sub></i> )-33				ca. -9.4·10 <sup>-3</sup> (410)	
	( <i>S<sub>s</sub></i> )-34	2	CHCl <sub>3</sub> (1·10 <sup>-3</sup> )	290	ca. -3.9·10 <sup>-3</sup> (375)	44
	( <i>R<sub>r</sub></i> )-34				ca. +3.9·10 <sup>-3</sup> (375)	
	( <i>S<sub>s</sub></i> )-35	67	CHCl <sub>3</sub> (1·10 <sup>-5</sup> )	n.a.	-6.0·10 <sup>-4</sup> (540)	45
	( <i>S<sub>s</sub></i> )-36	55	CHCl <sub>3</sub> (1·10 <sup>-5</sup> )	n.a.	+7.0·10 <sup>-4</sup> (540)	45
	( <i>R<sub>p</sub></i> )-41	51	CH <sub>2</sub> Cl <sub>2</sub> (1·10 <sup>-5</sup> )	ca. 360	Silent	46
<hr/>						
Other designs						
	Calycanthine	n.a.	EtOH (n.a.)	n.a.	+8·10 <sup>-3</sup> (ca. 350)	25
	( <i>R<sub>r</sub></i> )-9	48	CH <sub>2</sub> Cl <sub>2</sub> (n.a.)	366	+0.94·10 <sup>-3</sup> (ca. 546)	34
	( <i>R<sub>p</sub></i> )-22	46	CHCl <sub>3</sub> (1·10 <sup>-3</sup> )	529	+0.7·10 <sup>-3</sup> (550)	41
	( <i>S<sub>d</sub></i> )-22				-0.8·10 <sup>-3</sup> (550)	
	( <i>S<sub>p</sub></i> )-23	46	CHCl <sub>3</sub> (1·10 <sup>-5</sup> )	314	+1.1·10 <sup>-3</sup> (ca. 450)	42a
	( <i>R<sub>p</sub></i> )-23	46		300	-1.4·10 <sup>-3</sup> (418)	42b
	( <i>S<sub>p</sub></i> )-24	45	CHCl <sub>3</sub> (1·10 <sup>-5</sup> )	314	-1.1·10 <sup>-2</sup> (ca. 450)	42a
	( <i>R<sub>p</sub></i> )-24	41	CHCl <sub>3</sub> (1·10 <sup>-6</sup> )		+1.3·10 <sup>-2</sup> (453)	42b

$[\alpha]_{TFF}$  = trifluoroethanol